Spatio-temporal variations in COVID-19 in relation to the global climate distribution and fluctuations

Olaniran Jonathan Matthew[a], Adebayo Oluwole Eludoyin[b,*], Kehinde Sunday Oluwadiya[c]

[a] *Institute of Ecology and Environmental Studies, Obafemi Awolowo University, Ile-Ife, Nigeria*
[b] *Department of Geography, Obafemi Awolowo University, Ile-Ife, Nigeria*
[c] *Department of Surgery, Ekiti State University, Ado-Ekiti, Nigeria*

ARTICLE INFO

ABSTRACT

This study investigated the spatio-temporal variations in the occurrence of COVID-19 (confirmed cases and deaths) in relation to climate fluctuations in 61 countries, scattered around the world, from December 31, 2019 to May 28, 2020. Logarithm transformation of the count variable (COVID-19 cases) was used in a multiple linear regression model to predict the potential effects of weather variables on the prevalence of the disease. The study revealed strong associations ($-0.510 \leq r \leq -0.967$; $0.519 \leq r \leq 0.999$) between climatic variables and confirmed cases of COVID-19 in majority (68.85%) of the selected countries. It showed evidences of 1 to 7-day delays in the response of the infection to changes in weather pattern. Model simulations suggested that a unit fall in temperature and humidity could increase (0.04–18.70%) the infection in 19.67% and 16.39% of the countries, respectively, while a general reduction (-0.05 to 9.40%) in infection cases was projected in 14.75% countries with a unit drop in precipitation. In conclusion, the study suggests that effective public health interventions are crucial to containing the projected upsurge in COVID-19 cases during both cold and warm seasons in the southern and northern hemispheres.

© 2021 Elsevier Ltd. All rights reserved.

1. Introduction

In rapid succession, the first COVID-19 case (a severe acute respiratory syndrome coronavirus 2), which was first reported on December 31, 2019 in the city of Wuhan, China, has caused an outbreak of human-to-human transmission globally. The disease was declared a Public Health Emergency of International Concern (PHEIC) on January 30, 2020 and then a pandemic on March 11, 2020 by the World Health Organization, WHO (Chan et al., 2020; Lai et al., 2020; Li et al., 2020). Since the inception of the disease, concerted efforts have been made to have a better understanding of the genomics, hosts, modes of transmission and epidemiological link of the disease (Sahu et al., 2020). Previous studies have revealed that a significant number of respiratory infectious diseases display seasonal patterns in their incidence. However, the impact of climate variability and other extrinsic factors on COVID-19 transmission is still a subject of debate.

Climate is one of many factors likely affecting the spread of the virus (Briz-Redón and Serrano-Aroca, 2020; Di Pietro et al., 2020; Mishra and Wargocki, 2020) and that the host's behaviour

(Kraemer et al., 2019) and population density (Geoghegan and Holmes, 2017) are important predictors of the capacity of the virus to spread (Araujo and Naimi, 2020). Recent studies suggested that infected humans can be asymptomatic and transmit the virus to others, generating substantial uncertainties regarding the overall risk of epidemic outbreaks under a variety of different climate, ecological and social settings (Li et al., 2020). Specifically, Araujo and Naimi (2020) submitted that immediate physical environment can mediate human-to-human transmission of COVID-19 and that unsuitable climates can cause the virus to destabilize quickly, hence reducing its capacity to become epidemic. Further, the strong association of COVID-19 to a sharp North/South climate gradient, with a faster spread in warm and cold temperate climates have been reported (Araujo and Naimi, 2020; Briz-Redón and Serrano-Aroca, 2020; Di Pietro et al., 2020; Méndez-Arriaga, 2020). Similarly, Mishra and Wargocki (2020), Sajadi et al. (2020) and Wang et al. (2020a) suggested a close relationship between the incidence of COVID-19 epidemics and climate with countries in high latitudes (characterized by temperate and/or continental climate) exhibiting a high incidence of the disease. On the other hand, Briz-Redón and Serrano-Aroca (2020) and O'Reilly et al. (2020) stressed that since local transmission of the disease has been confirmed to span all climatic zones, further studies on the impact of climate

---

* Corresponding author.
  E-mail address: oaeludoyin@oauife.edu.ng (A.O. Eludoyin).

variability, on COVID-19 transmission is vital to increase understanding of the factors underlying the spread of the disease across the globe. Also, scholars have argued that atmospheric pollution could significantly contribute to the anomalous variability of COVID-19 depending on concentrations and chronicity of exposure (Conticini et al., 2020; Fattorini and Regoli, 2020; Zhu et al., 2020).

Owing to the introduction of lockdown measures (including transportation, businesses, and industrial shutdowns) by governments around the world to limit the COVID-19 pandemic, air quality has improved significantly in major cities of the world (Bashir et al., 2020). This is because reduced fossil fuel consumption will lower emissions into the atmosphere resulting in cleaner air (Sharif et al., 2020). About 20–50% in greenhouse gas emissions (e.g. CO_2, O_3, NO_x and SO_x) or/and other air pollutants (such as PM2.5, PM10, BC and benzene) in Korea, China, Spain, Germany, Italy, USA and New York compared to pre-epidemic years were reported in the literature (Collivignarelli et al., 2020; Conticini et al., 2020; Gautam, 2020; Knowland et al., 2020; Wang et al., 2020b). It has been argued that resumption of large-scale industrial activities after the epidemic will probably reverse the environmental changes, once the epidemic is controlled (Bashir et al., 2020; Bernauer and Slowey, 2020).

Previous studies suggested that people under lockdown will more likely develop psychological problems like stress disorders, fear, depression, emotional fatigue, and insomnia than people who freely move (Brooks et al., 2020; Fofana et al., 2020). Fattorini and Regoli (2020), thus, argued that environmental control should be integrated with human health protection into sustainable development as measures for controlling epidemics, on a long-term projection rather than a short-term, incidence-based measure. As new cases of COVID-19 are being confirmed daily around the world, there is a heightened concern, and pressure is mounting on researchers from various fields of study to improve our understanding of the factors underlying the spread of the disease. Some pertinent questions at the moment for COVID-19 mitigation strategies are: (i) Will the virus be less transmissible in hot and humid climates? (ii) Will changes in weather affect the transmission intensity of COVID-19? And (iii) will asynchronous seasonal global outbreaks occur in future if the spread of the disease continues to follow the current trend? The present study, therefore, investigates potential effects of spatio-temporal variations in world's geographical climate (in terms of humidity, temperature and precipitation) on the COVID-19 occurrence (incidence rate and prevalence rate) and its fatality rate. The study is designed to uncover certain underlying trends on the spread of COVID-19 concerning climate variability and link the results with findings from related previous researches with a view to providing useful information on the vulnerability of different climatic regions of the world to COVID-19 infection that could help to curtail its spread.

2. Methods

2.1. Data

Laboratory-confirmed infection case series of daily local transmissions of COVID-19 across the globe from the date of first reported case till May 28, 2020 (12.00 GMT) were obtained from https://ourworldindata.org/coronavirus; https://covid19info.live/. The website contained the worldwide country by country and regional COVID-19 data on many aspects of the disease such as the number of infections and death and other epidemiological and surveillance records. In addition, global climate data (hourly time-series of temperature, humidity, and precipitation) of high-resolution ERA5 datasets (freely available at https://cds.climate.copernicus.eu/#!/home) were obtained and analysed. ERA5 reanalysis is the fifth generation of atmospheric reanaly-

sis of the global climate developed by the European center for Medium-Range Weather Forecasts (ECMWF). It combines model data with observations from across the world into a globally complete and consistent dataset using the laws of physics with horizontal resolution of 0.25° × 0.25° (Copernicus Climate Change Service, 2017).

2.2. Statistical analysis and procedures

We analysed laboratory-confirmed infection case series of daily local transmissions of COVID-19 in 61 countries (representing 33.7% of countries with available COVID-19 data) in Asia, Oceania, Europe, North and South America, Arctic region and Africa from the date of first reported case in each country till May 28, 2020. Similarly, daily means of the climatic parameters over the selected countries during the study period were estimated. In order to ensure that the datasets that were analysed were valid and of good quality, data cleaning process was performed on both datasets to remove missing values. The local transmission ratio (LTR), defined by Méndez-Arriaga (2020) as the number of confirmed positive cases divided by the number of the effective contagion days since community onset of the disease, was estimated.

Multiple regression analysis and lag correlation (0–7 days) were performed to examine the association or relationship between the daily meteorological parameters i.e. temperature/°C, relative humidity/% and precipitation/mm (as independent variables) and COVID-19 cases (dependent variable). Before fitting linear regression models and correlation, we first subjected the data to statistical test for collinearity among the variables and normality as suggested by Zar (1992). As expected, the dependent variable (a count variable that did not conformed to these assumption) was transformed (using logarithm transformation) while the outliers (elements that are greater than the 3 scaled median absolute deviation (MAD) away from the median) that could introduce substantial errors in the outcomes of the analysis, were removed or smoothened (using MATLAB® command "filloutliers", version 2019a) before further analysis.

The variance stabilizing logarithm-transformation was performed on the dependent variable, Y as a function of time, t (days) using Eq. (1) as fully described in Feng et al. (2014) and Rodríguez-Barranco et al. (2017):

$$\log (Y_t) = \beta + \beta_1 X_{t1} + \beta_2 X_{t2} + \beta_3 X_{t3} + \in \tag{1}$$

where β was the y-intercept, $\beta_{i=1,2,3}$ were the regression coefficients for the three independent variables (temperature, humidity, and precipitation) respectively and $\in$ was the random error

Global spatial variations in monthly means of the three meteorological parameters between December 2019 and May 2020 were obtained and presented. In addition, changes in monthly means of these parameters relative to December 2019 (the month the first case of the disease was reported in China) were evaluated. Spatial patterns of confirmed COVID-19 cases were visualised by plotting their logarithmic values across different locations using the open access Paleontological Statistics (PAST3, version 3.12; Hammer et al., 2001) software. We adopted kriging interpolation algorithm (which accounts for uncertainties due to associated fit parameters in semivariogram as documented in Davis (1986) and de Smith et al. (2018)) for the 'gridding' (interpolation of scattered 2D data points onto a regular grid) operation. Furthermore, the potential effects of a unit change in the values of meteorological parameters on the spread of the infections in different regions of the world were also predicted. We used the findings from related previous studies on the roles of non-climatic factors in the global spread of COVID-19 to explain the patterns of results obtained in this present studies. Finally, possible effective methods of contain-
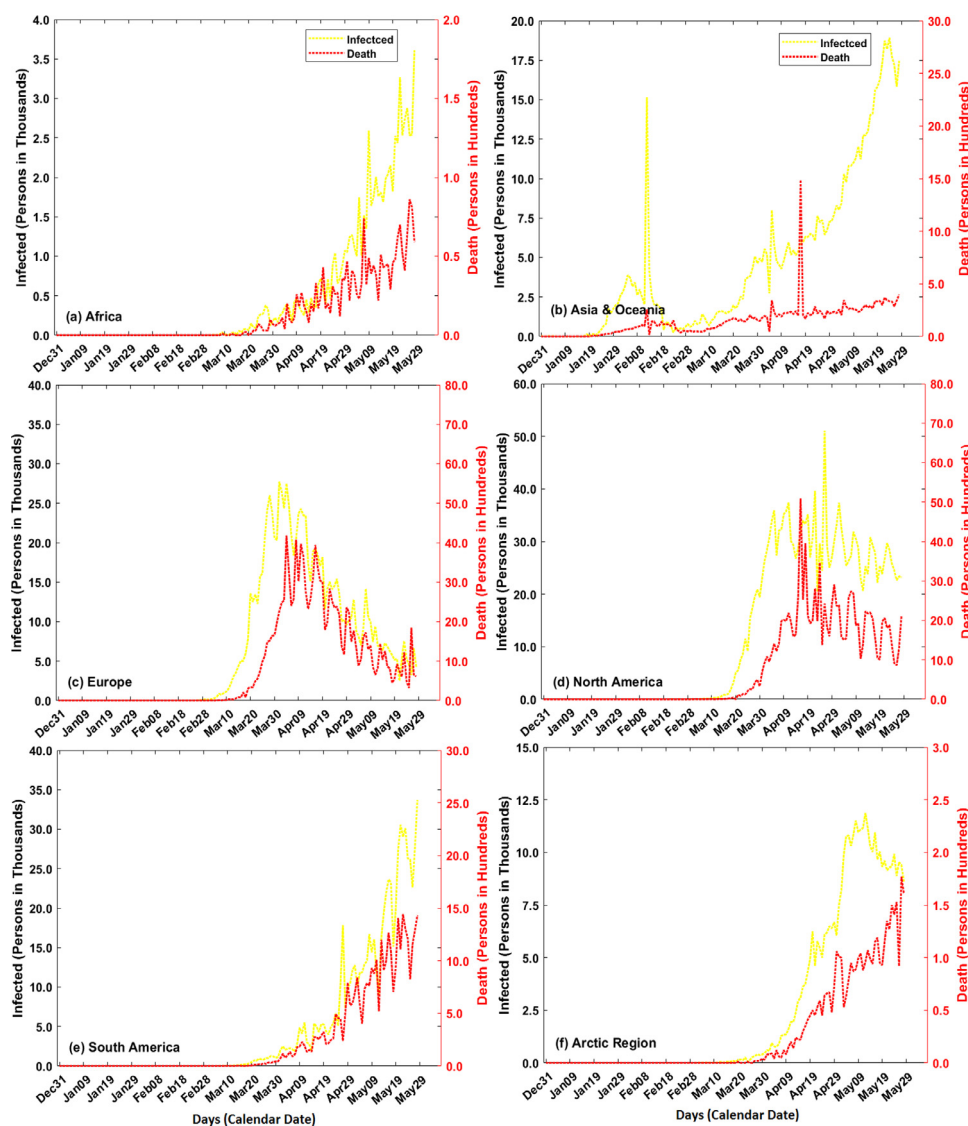
Fig. 1. COVID-19 confirmed and death cases in the 61 selected countries in (a) Africa, (b) Asia and Oceania, (c) Europe (d) North America, (e) South America, and (f) the Arctic Region from December 31, 2019 to May 28, 2020 at 12.00 GMT (*left vertical axis for the number of infected cases while right vertical axis is for the number of death*).

ment of the disease in different countries and regions were suggested based on results of the model simulations.

3. Results

3.1. Daily and spatial (monthly) variations in COVID-19 confirmed and death cases

Fig. 1 shows variation in the number of infection and death from COVID in the designated six regions of the world (i.e. Africa, Artic region, Asia & Oceania, Europe, North America, and South America). The results demonstrated that while Asia reported an outbreak of the disease around January 2020, the rest of the world did not report such until March 2020. Interestingly, Europe and North America consequently experienced more dramatic changes in the number of infection and fatality, but the rest of the world witnessed more gradual increases during the period. The results show a sharp rise in the number of cases and deaths from March 2020, with both outcomes peaking sometime in April over Europe and North America. In other regions, however, the number of infected individuals and fatalities recorded were found to continue to rise from March/April till the end of the study period. The total re-

ported cases during the study period were 1870,835 (North America); 1016,034 (Europe); 709,329 (South America); 694,471 (Asia & Oceania); 387,723 (Arctic region) and 74,819 (Africa). Similarly, the total fatality recorded in the six regions were 124,241 (Europe); 116,015 (North America); 35,063 (South America); 22,184 (Asia); 4057 (Arctic region) and 1971 (Africa). Fig. 2 describes the monthly spatial (along the latitude and longitude) spread of the infection from the epicentre from December 2019 to May 2020. Globally, the spread of the disease was more pronounced in the northern hemisphere and the prominent direction of the transmission was from China to the western countries.

Estimated local transmission ratio (LTR) for each of the countries scattered over different regions are presented in Fig. 3. In Africa, LTR values ranged between about 371 and 2 persons day^{-1} (Fig. 4a). South Africa had the highest closely followed by Egypt (LTR = 275 persons day^{-1}) while the least was recorded in Zimbabwe. India (LTR = 1070 persons day^{-1}) and Iran (LTR = 957 persons day^{-1}) were the highest in Asia & Oceania while New Zealand (LTR = 2 persons day^{-1}) was the lowest (Fig. 4b). In Europe, United Kingdom had the highest LTR (2365 persons day^{-1}) closely followed by Spain (2095 persons day^{-1}) while Norway (74 persons day^{-1}) and Bulgaria (22 persons day^{-1}) were the lowest
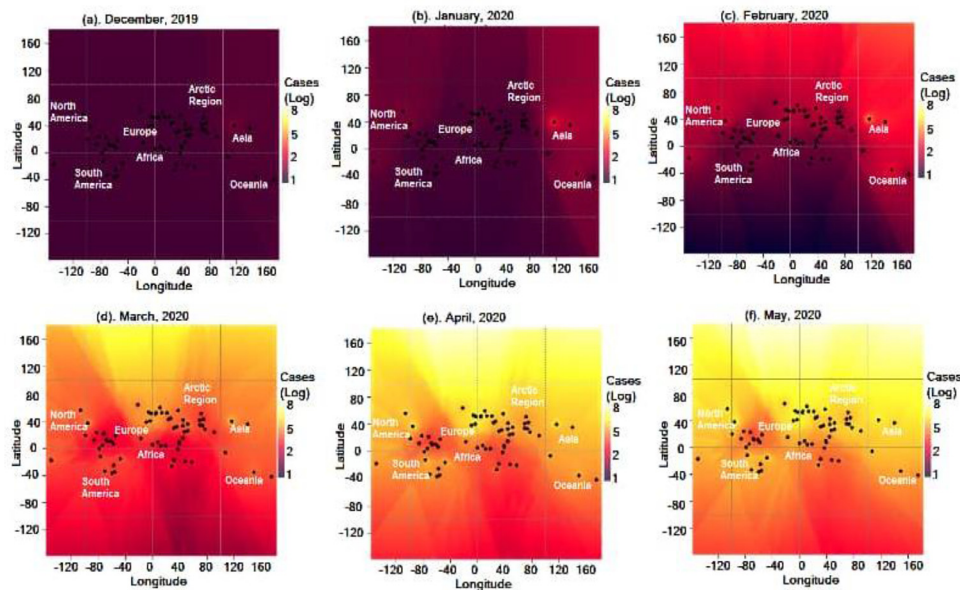
Fig. 2. Spatial plot of log of COVID-19 confirmed cases in (a) December 2019, (b) January, (c) February (d) March, (e) April, and (f) May, 2020 (*the black dots represent the 61 selected countries around the world*).

(Fig. 4c). The USA in North America, Brazil in South America and Russia in the Arctic region had the highest LTR of 23,943, 5280 and 3280 persons day^{-1} respectively. The results revealed that North American countries had the highest LTR of 26,334 persons day^{-1}. Next was Europe (8991 persons day^{-1}), closely followed by South America (9108 persons day^{-1}), Asia (4692 persons day^{-1}), and the Arctic Region (3421 persons day^{-1}) while Africa came last with LTR of 1069 persons day^{-1} respectively (See supplementary Fig. 1).

3.2. Daily variations in weather conditions and mean monthly climatology

The estimated global monthly climatology of surface air temperature (°C), relative humidity (%) and total precipitation (mm) for December 2019 in China are depicted in Fig. 4. It showed relatively warmer climate (20–40 °C) in the tropics (25°N–25°S) but colder climate (−60 - +19 °C) in the higher latitudes in the north (e.g. parts of Artic region, Europe, northern Africa, Asia and North America) and southern hemispheres (e.g. parts of South America, Oceania and southern Africa) (Fig. 4a). The Arctic (e.g. Georgia, Iceland, Kyrgyzstan, Kazakhstan, Russia and Uzbekistan) and Oceania (e.g. Australia and New-Zealand) regions were extremely cold (< −30 °C) during this period. Furthermore, most parts of the word were very humid with relative humidity greater than 50% (Fig. 4b). However, some islands in the Pacific, India, and Atlantic oceans, as well as a few places in Far East Asia (e.g. Bangladesh, China and India), had very low relative humidity between 10 and 40%. The most humid inland regions (with humidity $\geq$ 80%) were found in the tropics and northern hemisphere. In addition, wet regions (with records of precipitation $\geq$ 10 mm) were found in the tropical parts of western (e.g. Nigeria, Senegal, Ghana) and southern Africa (e.g. Mauritius, Zimbabwe), southern Asia & Oceania (e.g. Indonesia, Australia and New-Zealand); southern parts of North America (e.g. Mexico) as well as South America (e.g. Argentina, Brazil, Ecuador, Paraguay, Peru and Uruguay) (Fig. 4c). During this month, most parts of Europe, Asia, North America, and the Oceania were very dry. Fig. 5 presents changes in global monthly climatology of temperature, humidity and precipitation in the months of March and April 2020 (relative to December 2019). Results revealed general

decrease in temperature between December 2019 and March 2020 in the Arctic Region (−5 to −27 °C), Oceania (−2 to −10 °C), parts of Europe (−2 to −10 °C), Asia (−2 to −10 °C), South and North America (−2 to −10 °C), and southern Africa (−2 to −10 °C).The area with the highest warming (10–15 °C rise in temperature) was found in the southern coast of South America (Fig. 5a). The temperature decreased further in April with more areas around the world getting colder while the South Pole and southern coast of South America became warmer. Relative humidity was found to increase (5–40%) in warmer regions and decreased (−5 to −40%) in a colder region (Fig. 5b).Similarly, there were further increase and decrease in relative humidity in the month of April. Notably are the South Pole, Oceania parts of Asia and North America with higher humidity. Apart from parts of southern Asia with significant increase and decrease in wetness (± 40 mm), other regions showed a slight, albeit insignificant, increase or decrease in precipitation in March and April 2020 (Fig. 5c).

3.3. Relationship between variations in COVID-19 infections and weather conditions

Scattered plot of COVID-19 cases in relation to selected weather parameters indicate non-normal distribution and erratic linear patterns between new daily COVID-19 cases and the parameters (Supplementary Fig. 2). The logarithm-transformation of the dependent variable and removal of outliers, nonetheless, produced acceptable normal distribution and collinearity among the variables required for regression analysis as done in this study. Consequently, the lagged correlation coefficient at 0 to 7-days period was evaluated to ascertain the level of weather-COVID-19 daily occurrences (Tables 1–6). The coefficients reveal strong (positive and negative) relationships between the weather parameters and COVID-19 infections in about 67.2% of the selected countries. Strong and positive correlation coefficients were obtained between (new) reported cases and temperature in two African countries i.e. Egypt and Ethiopia (Table 1), as well as in some Asia countries (Bangladesh, India, Indonesia, Iran, Iraq, Pakistan, Qatar, Saudi Arabia and Yemen; Table 2), Europe (Bulgaria, United Kingdom, Poland, and Romania; Table 3), North America (Canada, Mexico, Cuba and the

Table 1
Lagged correlation coefficients at 0 to 7-days between the daily reported infected cases and temperature (TMP in °C), relative humidity (RHU in %) and precipitation (PRE in mm) over selected countries in Africa (* *significant at* *p ≤ 0.05; bold value is an indicator of lagging*).

Parameter	Lag/days	Countries												
		Cameroon	CAR	Egypt	Ethiopia	Ghana	Kenya	Madagascar	Mauritius	Nigeria	South Africa	Senegal	Tanzania	Zimbabwe
TMP	0	−0.097	−0.166	0.905*	0.617*	−0.510*	−0.823*	−0.601*	0.019	−0.074	−0.962*	−0.385	−0.040	−0.397
	1	−0.056	−0.144	0.948*	0.614*	−0.518*	−0.805*	−0.538*	0.030	−0.057	−0.961*	−0.390	0.043	−0.371
	2	−0.104	−0.154	0.978*	0.565*	−0.468	−0.808*	−0.552*	0.031	−0.052	−0.967*	−0.399	−0.032	−0.392
	3	−0.101	−0.134	0.999*	0.519*	−0.501*	−0.812*	−0.630*	0.014	−0.044	−0.966*	−0.446	0.011	−0.345
	4	−0.086	−0.126	0.999*	0.580*	−0.453	−0.786*	−0.635*	0.033	−0.044	−0.952*	−0.512*	0.027	−0.401
	5	−0.061	−0.127	0.998*	0.606*	−0.405	−0.775*	−0.575*	0.039	−0.044	−0.960*	−0.568*	−0.010	−0.464
	6	−0.113	−0.162	0.980*	0.513*	−0.324	−0.748*	−0.557*	0.029	−0.022	−0.958*	−0.605*	−0.042	−0.421
	7	−0.050	−0.154	0.956*	0.441	−0.354	−0.736*	−0.558*	0.056	0.013	−0.965*	−0.629*	−0.040	−0.371
RHU														
	0	0.532*	0.368	−0.494	0.079	−0.647*	0.564*	−0.449	0.014	0.862*	−0.796*	0.656*	0.062	−0.401
	1	0.543*	0.376	−0.564*	0.063	−0.616*	0.574*	−0.445	0.049	0.880*	−0.778*	0.639*	0.014	−0.371
	2	0.553*	0.384	−0.588*	0.072	−0.562*	0.578*	−0.457	−0.016	0.896*	−0.771*	0.644*	0.096	−0.484
	3	0.551*	0.367	−0.615*	0.112	−0.558*	0.571*	−0.458	0.058	0.908*	−0.733*	0.656*	−0.010	−0.546
	4	0.549*	0.382	−0.620*	0.035	−0.533*	0.562*	−0.548*	−0.014	0.910*	−0.742*	0.681*	0.001	−0.480
	5	0.546*	0.390	−0.580*	0.043	−0.605*	0.556*	−0.531*	0.007	0.923*	−0.814*	0.677*	0.009	−0.408
	6	0.557*	0.401	−0.548*	0.158	−0.638*	0.551*	−0.578*	−0.048	0.908*	−0.812*	0.671*	0.110	−0.428
	7	0.561*	0.392	−0.506*	0.182	−0.595*	0.568*	−0.544*	0.002	0.891*	−0.801*	0.681*	0.051	−0.424
PRE														
	0	0.436	0.291	0.443	0.439	−0.593*	0.048	−0.423	0.030	0.652*	−0.823*	0.596*	0.097	−0.453
	1	0.443	0.282	0.514*	0.435	−0.574*	0.096	−0.397	−0.010	0.639*	−0.834*	0.644*	0.025	−0.446
	2	0.441	0.287	0.495	0.367	−0.597*	0.129	−0.361	−0.011	0.656*	−0.835*	0.676*	0.001	−0.455
	3	0.447	0.330	0.449	0.341	−0.594*	0.120	−0.395	−0.007	0.671*	−0.830*	0.682*	0.016	−0.437
	4	0.456	0.349	0.435	0.389	−0.583*	0.119	−0.427	−0.011	0.692*	−0.818*	0.638*	−0.014	−0.463
	5	0.459	0.330	0.428	0.383	−0.570*	0.126	−0.385	−0.043	0.707*	−0.830*	0.609*	0.039	−0.471
	6	0.452	0.285	0.392	0.296	−0.554*	0.142	−0.383	−0.015	0.717*	−0.835*	0.581*	0.056	−0.447
	7	0.434	0.324	0.341	0.273	−0.554*	0.177	−0.384	0.014	0.709*	−0.839*	0.579*	0.072	−0.429

Table 2

Lagged correlation coefficients at 0 to 7-days between the daily reported infected cases and temperature (TMP in °C), relative humidity (RHU in %) and precipitation (PRE in mm) over selected countries in Asia and Oceania (* significant at $p \leq 0.05$; *bold value is an indicator of lagging*).

| Parameter	Lag/days	Countries														
		Afghanistan	Bangladesh	China	India	Indonesia	Iran	Iraq	Israel	Japan	Pakistan	Qatar	S/Arabia	Yemen	Australia	N/Zealand
TMP	0	0.430	0.549*	−0.275	0.938*	0.453	0.682*	0.836*	0.262	0.199	0.771*	0.838*	0.858*	0.443	−0.113	−0.244
	1	0.405	0.560*	−0.284	0.931*	0.471	0.679*	0.847*	0.244	0.185	0.802*	0.839*	0.857*	0.446	−0.071	−0.238
	2	0.380	0.569*	−0.303	0.928*	0.535*	0.669*	0.856*	0.235	0.192	0.818*	0.838*	0.857*	0.484	−0.076	−0.236
	3	0.390	0.579*	−0.310	0.921*	0.551*	0.659*	0.834*	0.215	0.204	0.843*	0.837*	0.857*	0.513*	−0.053	−0.240
	4	0.349	0.591*	−0.329	0.920*	0.562*	0.660*	0.844*	0.194	0.182	0.837*	0.828*	0.859*	0.510*	−0.048	−0.200
	5	0.352	0.610*	−0.354	0.926*	0.553*	0.643*	0.858*	0.204	0.140	0.794*	0.817*	0.863*	0.538*	−0.051	−0.188
	6	0.343	0.627*	−0.356	0.936*	0.572*	0.634*	0.817*	0.207	0.119	0.789*	0.826*	0.870*	0.534*	−0.043	−0.220
	7	0.370	0.624*	−0.380	0.936*	0.484	0.649*	0.804*	0.206	0.141	0.778*	0.838*	0.877*	0.533*	−0.056	−0.241
RHU																
	0	−0.007	0.876*	0.397	−0.436	−0.623*	−0.218	−0.719*	−0.204	0.029	−0.354	−0.722*	−0.471	−0.223	0.064	0.342
	1	0.075	0.888*	0.384	−0.420	−0.560*	−0.181	−0.740*	−0.185	−0.038	−0.372	−0.709*	−0.455	−0.283	0.035	0.322
	2	0.110	0.891*	0.304	−0.408	−0.584*	−0.169	−0.715*	−0.187	−0.039	−0.411	−0.705*	−0.442	−0.365	−0.007	0.323
	3	0.137	0.893*	0.330	−0.385	−0.518*	−0.140	−0.716*	−0.167	−0.050	−0.425	−0.700*	−0.426	−0.373	−0.090	0.306
	4	0.126	0.891*	0.337	−0.355	−0.527*	−0.123	−0.687*	−0.127	0.014	−0.435	−0.670*	−0.404	−0.380	−0.079	0.282
	5	0.169	0.882*	0.392	−0.321	−0.492	−0.123	−0.700*	−0.168	0.063	−0.423	−0.648*	−0.372	−0.387	−0.089	0.203
	6	0.208	0.881*	0.417	−0.287	−0.511*	−0.095	−0.679*	−0.191	0.011	−0.415	−0.638*	−0.346	−0.355	−0.072	0.182
	7	0.240	0.893*	0.439	−0.253	−0.501	−0.091	−0.666*	−0.175	0.001	−0.440	−0.643*	−0.337	−0.357	−0.076	0.198
PRE																
	0	0.422	0.896*	−0.167	0.575*	−0.053	0.607*	0.466	0.108	0.086	0.518*	0.141	0.385	0.488	−0.135	−0.007
	1	0.402	0.918*	−0.194	0.591*	0.043	0.601*	0.450	0.037	0.037	0.527*	0.159	0.409	0.494	−0.111	−0.032
	2	0.460	0.935*	−0.226	0.592*	0.142	0.601*	0.380	0.107	0.057	0.522*	0.178	0.420	0.458	−0.177	−0.001
	3	0.454	0.943*	−0.217	0.603*	0.218	0.619*	0.340	0.103	0.058	0.550*	0.189	0.431	0.433	−0.188	−0.022
	4	0.412	0.931*	−0.216	0.626*	0.302	0.603*	0.363	0.115	0.051	0.554*	0.196	0.464	0.466	−0.166	−0.017
	5	0.471	0.903*	−0.241	0.695*	0.302	0.599*	0.380	0.130	0.090	0.531*	0.212	0.500*	0.436	−0.176	−0.026
	6	0.495	0.880*	−0.221	0.760*	0.244	0.566*	0.339	0.099	0.065	0.559*	0.260	0.524*	0.392	−0.155	−0.059
	7	0.561	0.874*	−0.218	0.803*	0.192	0.614*	0.352	0.075	0.062	0.581*	0.282	0.539*	0.395	−0.210	−0.093
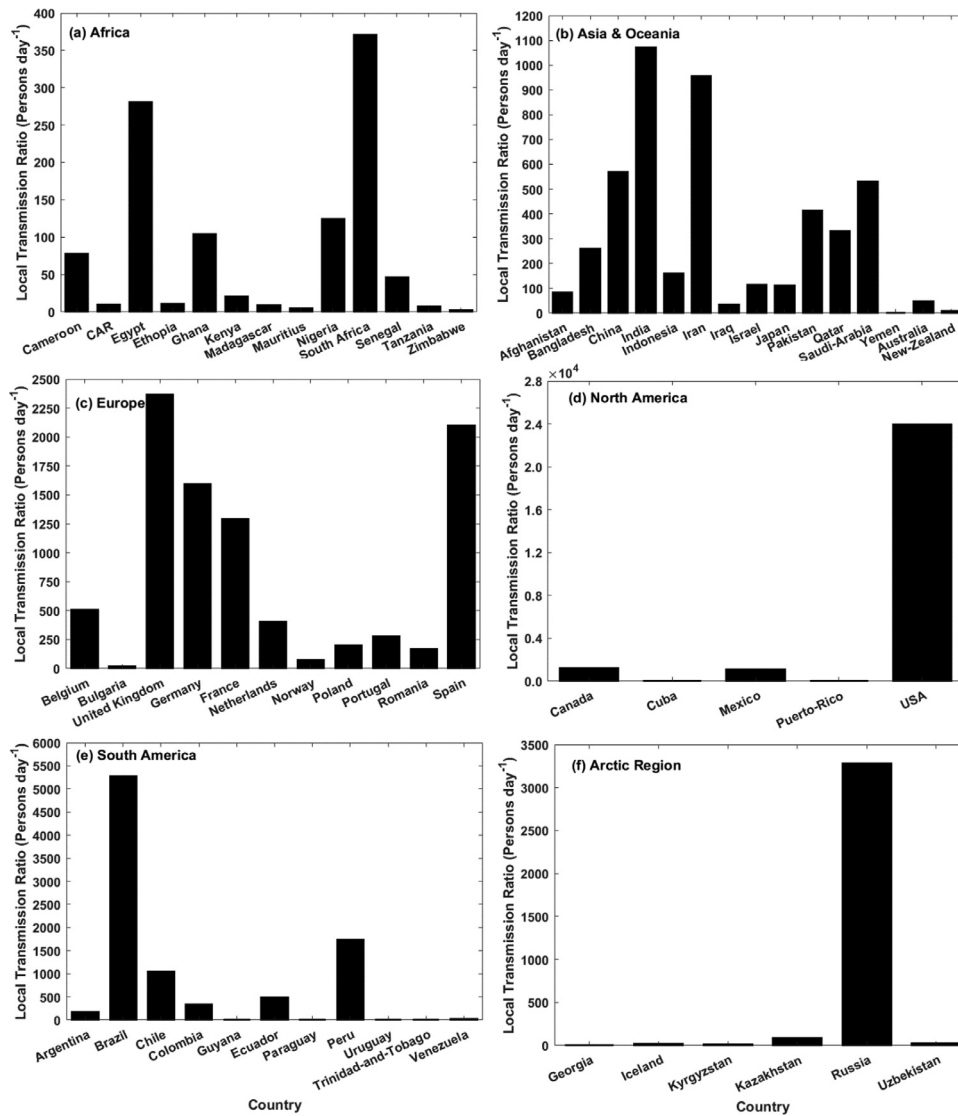
Fig. 3. Estimated Local Transmission Ratio (LTR) in different countries in (a) Africa, (b) Asia and Oceania, (c) Europe (d) North America, (e) South America, and (f) the Arctic Region from December 31, 2019 to May 28, 2020 at 12.00 GMT.

USA; Table 4), and the Arctic region (Kyrgyzstan, Russia; Table 5). Countries where correlations between COVID-19 cases and temperature were negative and significant (at $p < 0.05$) include: Ghana, Kenya, Madagascar, and South Africa in Africa (Table 1); and Argentina, Brazil, Chile, Paraguay and Peru in South America (Table 6). With respect to relative humidity, there was positive and significant relationship with COVID-19 infections in Cameroon, Nigeria, Kenya, and Senegal (Africa) and Bangladesh (Asia). The relationship was, however, negative ($-0.506 \leq r \leq -0.906$) but significant in Egypt, Ghana, Madagascar and South Africa (Africa); Indonesia, Iraq and Qatar (Asia); Belgium, Bulgaria, United Kingdom, Germany, France, Netherlands, Poland and Romania (Europe); Mexico (North America); as well as Brazil and Peru (South America). During the study period, precipitation had significant and positive correlations ($0.514 \leq r \leq 0.947$) with the (new) reported COVID-19 cases in Egypt, Nigeria and Senegal (Africa); Bangladesh, India, Iran and Pakistan (Asia); and Kyrgyzstan, Kazakhstan, Russia and Uzbekistan (Arctic region). However, this relationship was significantly negative ($-0.530 \leq r \leq -0.839$) in Ghana and South Africa (Africa), Brazil and Peru (South America).

In addition, some significant varying time-delay effects were obtained between climatic variables and COVID-19 infections. For

instance, time-lag between change in temperature and maximum occurrence of infection was 1-day in Canada (North America; Table 4) and Argentina (South Africa; Table 6). In addition, the results revealed 2-day lagging in Ghana and South Africa (Africa); Poland (Europe); Iran and Qatar (Asia); Mexico (North America); and Chile (North America). Three-day lagging was obtained in Egypt, Pakistan and Peru Madagascar recorded 4-day lagging. Yemen and Kyrgyzstan had 5-day lagging to temperature effects while Bangladesh and the USA had 6-day time lag. Similar wobbling results were obtained for relative humidity and precipitation with time-lags ranging between 1 and 7 days in 16 and 10 countries respectively.

3.4. Statistical simulations of COVID-19 infections in relation to changes in weather

Projected percentage changes in COVID-19 cases associated with a unit decrease in temperature (°C), relative humidity (%) and precipitation (mm) are illustrated in Fig. 6. Generally, our results suggested that one-degree Celsius drop in temperature will alter (increase or decrease) the number of COVID-
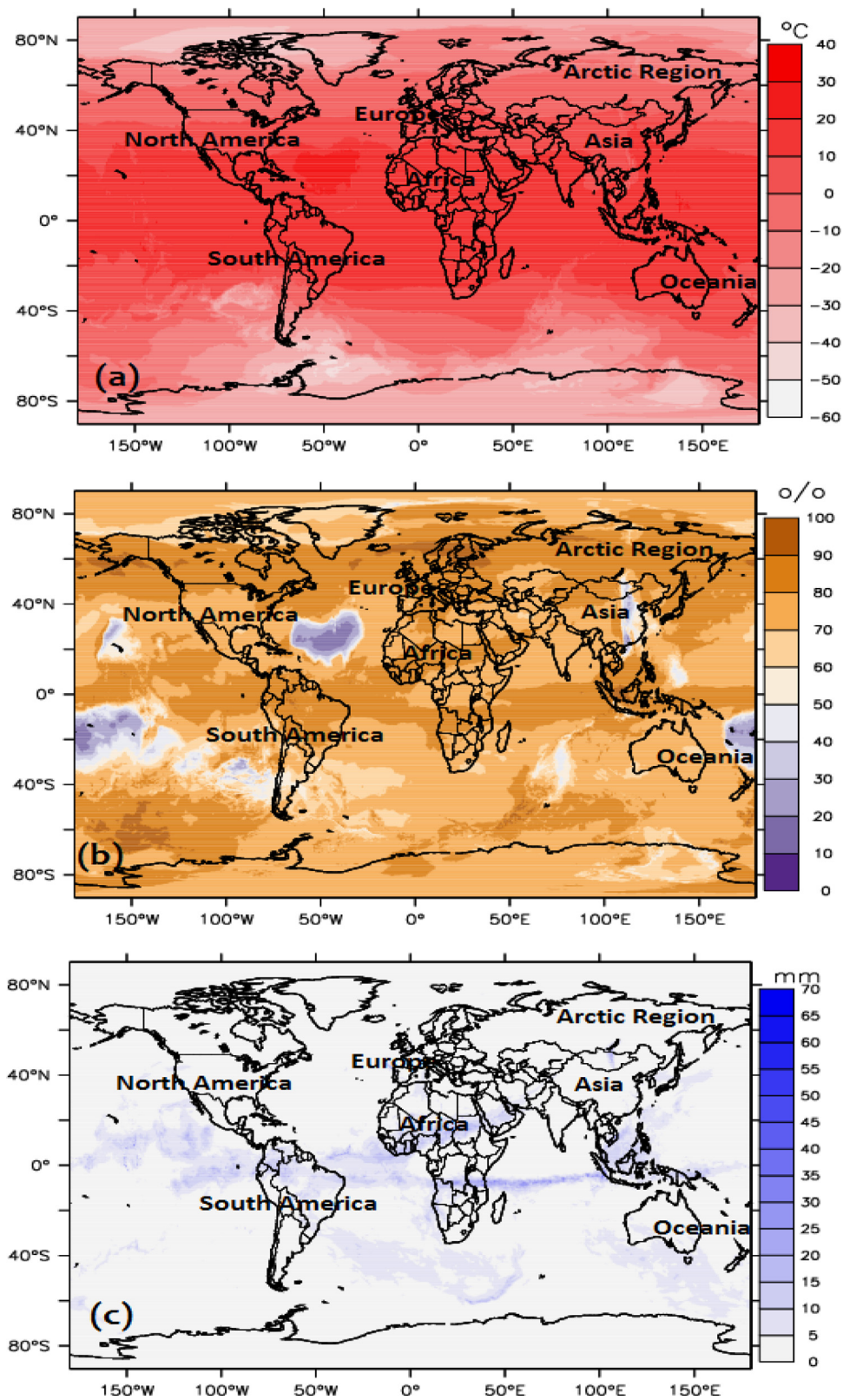
Fig. 4. Global monthly climatology of (a) surface air temperature, (b) relative humidity and (c) total precipitation for the month of December 2019 (The period when the first case was first confirmed).
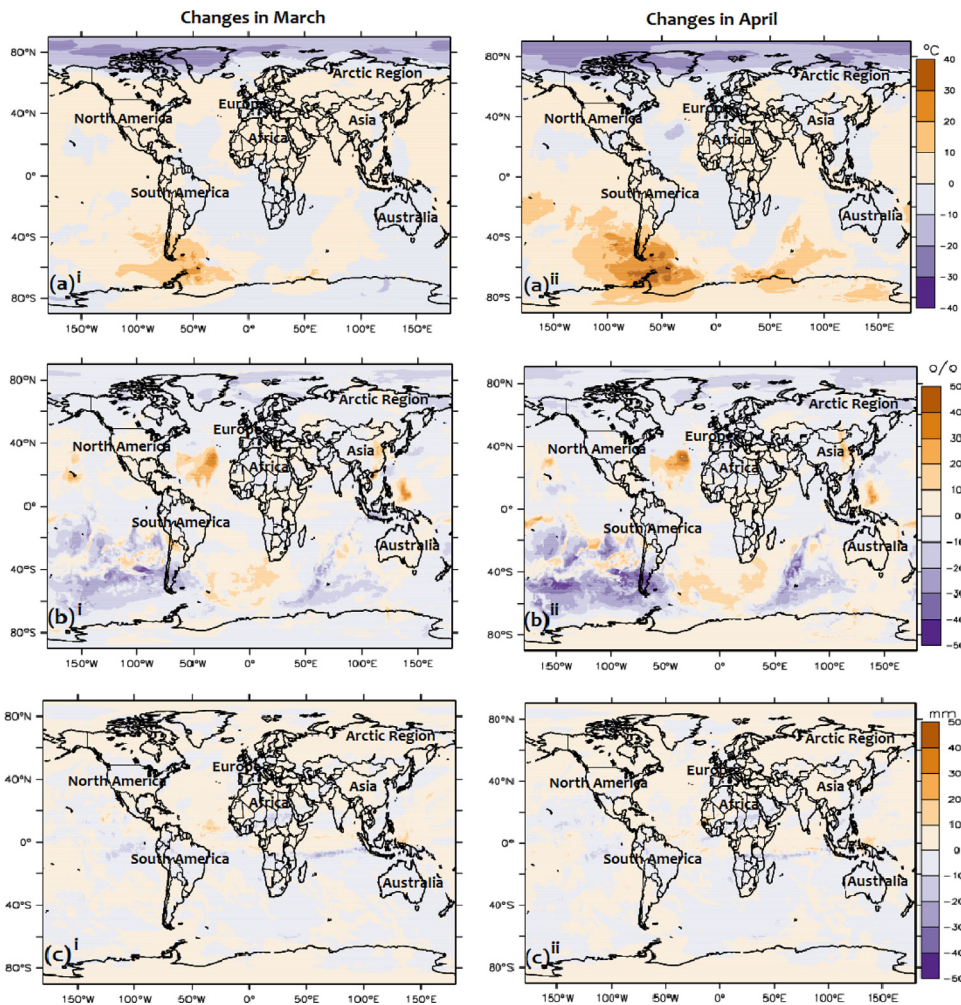
Fig. 5. Change in global monthly climatology of (a) surface air temperature, (b) relative humidity and (c) total precipitation in the months of March (left panel) and April (right panel) 2020 (The peak of the epidemic worldwide) relative to December, 2019.

19 cases significantly (at $p < 0.05$) in six countries in Africa including Ethiopia (14.10%), Egypt (−9.40%), Madagascar (1.40%), South Africa (1.60%), Kenya (−1.25), and Ghana (−2.70%; Fig. 6a). Similar results were obtained in one country, each, in Asia (Iraq = −4.50%; Fig. 6b), and Europe (Bulgaria = −18.70%; Fig. 6c) as well as five in North America (Canada = 0.16%, USA = 0.45%, Mexico = −0.63%, Puerto Rico = −1.42% and Cuba = 0.45%; Fig. 6d); Seven in South America (Peru = 2.20%,Paraguay = 0.71%, Brazil = 0.49%, Ecuador = 0.27%, Trinidad and Tobago =0.20%, Guyana = −0.12%, and Venezuela = −0.10%; Fig. 6e) and four in the Arctic region (Iceland = 0.55%, Georgia =0.15%, Kyrgyzstan = −0.37%, and Russia = −0.17%; Fig. 6f). For 1% drop in relative humidity, the model projected significant changes in three countries, each, in Africa (Ethiopia = 1.7%, Egypt = −2.5%, and Ghana = −1.3%), North America (USA = −0.1%, Mexico = 0.1%, and Puerto Rico = 0.07%) and Arctic region (Iceland =−0.11%, Kyrgyzstan = 0.04%, and Russia = 0.04%); two in Asia (Iraq = 1.2%; Pakistan = −0.4), 1 in Europe (Bulgaria = 7.2%); and four in South America (Peru =0.40%,Paraguay = 0.10%, Brazil = 0.15%, Ecuador =−0.14%). Finally, significant changes were obtained with 1 mm drop in two countries in North America (Canada = −0.09% and the USA = −0.07%), one country, each, in Asia (Pakistan = −0.05) and South America (Chile = −0.1%) and 5 in the Arctic region (Kyrgyzstan = −0.10%, Iceland = −0.09%, Georgia = −0.09%, Russia =−0.07% and Uzbekistan = −0.05%).

4. Discussion

The present study revealed that the total number of reported cases and death had reached 4753,211 and 303,531 respectively by the end of the study period (May 28, 2020) in all the selected 61 countries scattered over the globe. In order of severity of the disease, the North America (1.87 million cases) and Europe (1.02 million cases) were on top. They were followed by South America (709,329), Asia & Oceania (694,471), and the Arctic region (387,723) while Africa was in the rear with 74,819 confirmed cases. Mortalities from COVID-19 followed very similar pattern. The highest was recorded in Europe with 124,241 deaths closely followed by North America (116, 015 death) and then South America (35,063), Asia (22,184), Arctic region (4057) and Africa (1971). Results demonstrated that the order of the LTR from the highest to the lowest in the six regions is: North America (26,334 persons day^{-1}) - Europe (8991 persons day^{-1}) - South America (9108 persons day^{-1}) - Asia (4692 persons day^{-1}) - Arctic region (3421 persons day^{-1}) – Africa (1069persons day^{-1}).

Results of spatial distribution of the infections suggested that spread of the disease was highest in the northern hemisphere (i.e. high latitudes, with temperate and/or continental climate) and the prominent direction of the transmission was mainly from the epicentre to Europe and North America; mimicking the popular travel patterns from China. Previous studies have reported that no-

Table 3

Lagged correlation coefficients at 0 to 7-days between the daily reported infected cases and temperature (TMP in °C), relative humidity (RHU in%) and precipitation (PRE in mm) over selected countries in Europe (* significant at p ≤ 0.05; bold value is an indicator of lagging).

Parameters	Lag/days	Countries										
		Belgium	Bulgaria	U/Kingdom	Germany	France	Netherlands	Norway	Poland	Portugal	Romania	Spain
TMP	0	0.454	0.668*	0.677*	0.127	−0.087	0.329	−0.051	0.769*	0.143	0.700*	0.069
	1	0.432	0.636*	0.642*	0.112	−0.095	0.317	−0.079	0.756*	0.144	0.654*	0.077
	2	0.390	0.606*	0.528*	0.076	−0.111	0.293	−0.072	0.775*	0.112	0.631*	0.094
	3	0.367	0.569*	0.495*	0.040	−0.111	0.272	−0.044	0.741*	0.107	0.628*	0.105
	4	0.342	0.542*	0.543*	0.025	−0.132	0.256	−0.057	0.723*	0.111	0.633*	0.107
	5	0.326	0.534*	0.556*	−0.002	−0.134	0.242	−0.214	0.704*	0.095	0.643*	0.101
	6	0.289	0.535*	0.576*	−0.009	−0.147	0.238	−0.263	0.667*	0.113	0.631*	0.113
	7	0.302	0.528*	0.622*	0.003	−0.167	0.226	−0.154	0.643*	0.072	0.593*	0.160
RHU	0	−0.861*	−0.607*	−0.654*	−0.650*	−0.663*	−0.850*	−0.226	−0.871*	0.243	−0.720*	0.246
	1	−0.857*	−0.569*	−0.646*	−0.639*	−0.604*	−0.832*	−0.285	−0.890*	0.249	−0.709*	0.247
	2	−0.849*	−0.557*	−0.644*	−0.650*	−0.532*	−0.832*	−0.283	−0.906*	0.227	−0.688*	0.244
	3	−0.885*	−0.518*	−0.613*	−0.628*	−0.512*	−0.852*	−0.247	−0.901*	0.272	−0.661*	0.216
	4	−0.923*	−0.472	−0.639*	−0.654*	−0.533*	−0.873*	−0.232	−0.892*	0.274	−0.637*	0.194
	5	−0.857*	−0.466	−0.626*	−0.634*	−0.516*	−0.868*	−0.336	−0.903*	0.226	−0.660*	0.189
	6	−0.795*	−0.459	−0.623*	−0.588*	−0.460	−0.827*	−0.237	−0.920*	0.243	−0.685*	0.172
	7	−0.814*	−0.433	−0.642*	−0.547*	−0.449	−0.779*	−0.135	−0.899*	0.183	−0.655*	0.129
PRW	0	−0.100	0.387	0.139	−0.345	−0.270	−0.318	−0.226	0.088	0.183	0.316	0.182
	1	−0.099	0.358	0.058	−0.330	−0.254	−0.317	−0.224	0.111	0.155	0.276	0.192
	2	−0.160	0.323	−0.011	−0.365	−0.181	−0.306	−0.225	0.087	0.171	0.254	0.208
	3	−0.178	0.315	0.015	−0.365	−0.170	−0.329	−0.202	0.072	0.184	0.266	0.234
	4	−0.218	0.343	0.044	−0.388	−0.179	−0.353	−0.142	0.081	0.172	0.295	0.216
	5	−0.227	0.359	0.019	−0.417	−0.194	−0.366	−0.278	0.077	0.177	0.276	0.197
	6	−0.198	0.344	0.063	−0.397	−0.222	−0.351	−0.335	0.000	0.177	0.228	0.193
	7	−0.181	0.340	0.085	−0.356	−0.230	−0.335	−0.212	−0.003	0.142	0.205	0.222

Table 4

Lagged correlation coefficients at 0 to 7-days between the daily reported infected cases and temperature (TMP in °C), relative humidity (RHU in %) and precipitation (PRE in mm) over selected countries in North America (* significant at p ≤ 0.05; bold value is an indicator of lagging).

Parameters	Lag/days	Countries				
		Canada	Cuba	Mexico	Puerto-Rico	USA
TMP	0	0.766*	0.674*	0.660*	0.590*	0.619*
	1	0.773*	0.651*	0.664*	0.519*	0.623*
	2	0.756*	0.650*	0.668*	0.501	0.628*
	3	0.755*	0.658*	0.667*	0.487	0.613*
	4	0.737*	0.651*	0.663*	0.453	0.615*
	5	0.747*	0.637*	0.654*	0.449	0.620*
	6	0.739*	0.620*	0.643*	0.449	0.638*
	7	0.737*	0.611*	0.634*	0.412	0.614*
RHU	0	−0.134	0.009	−0.627*	−0.126	−0.092
	1	−0.091	0.018	−0.607*	−0.120	−0.090
	2	−0.097	0.034	−0.592*	0.012	−0.080
	3	−0.142	0.061	−0.577*	0.083	−0.113
	4	−0.119	0.008	−0.568*	0.027	−0.086
	5	−0.096	0.001	−0.559*	−0.081	−0.082
	6	−0.090	−0.009	−0.549*	0.008	−0.024
	7	−0.106	−0.016	−0.538*	0.044	−0.034
PRE	0	0.318	0.158	−0.042	0.165	0.367
	1	0.346	0.178	0.060	0.172	0.358
	2	0.317	0.198	0.141	0.148	0.361
	3	0.323	0.179	0.211	0.164	0.348
	4	0.322	0.180	0.247	0.176	0.353
	5	0.307	0.176	0.253	0.148	0.352
	6	0.306	0.176	0.241	0.117	0.379
	7	0.320	0.154	0.229	0.098	0.360

table countries to the west of China (such as Malaysia, the Philippines, Indonesia, and Thailand in Asia; major hubs in Europe, the US and Australia; Paraguay in South America as well as Burkina Faso and the Democratic Republic of the Congo in Africa) were the popular travel destinations from China before Wuhan's lockdown (Lai et al., 2020; O'Reilly et al., 2020). However, the pattern of results obtained in the present study did not wholly conform to the observed travel patterns. This is probably because travel patterns alone are not the only variables responsible for the spread of the disease. Country specific factors such as early imposition of lockdown, enforcement of other virus containing measures and environmental factors like intensity of sunlight which is important in the synthesis of Vitamin D in the body may play important roles. Vitamin D has been found to be protective of infections from coronaviruses including COVID-19 (Chakrabarti et al., 2020).

Table 5

Lagged correlation coefficients at 0 to 7-days between the daily reported infected cases and temperature (TMP in °C), relative humidity (RHU in %) and precipitation (PRE in mm) over selected countries in the Arctic region (* *significant at* $p \leq 0.05$; *bold value is an indicator of lagging*).

Parameters	Lag/days	Countries					
		Georgia	Iceland	Kyrgyzstan	Kazakhstan	Russia	Uzbekistan
TMP	0	0.387	−0.283	0.758*	−0.006	0.856*	0.375
	1	0.363	−0.309	0.725*	−0.083	0.832*	0.388
	2	0.346	−0.299	0.687*	−0.059	0.819*	0.388
	3	0.340	−0.300	0.715*	−0.062	0.811*	0.372
	4	0.330	−0.297	0.764*	−0.068	0.804*	0.410
	5	0.354	−0.260	0.777*	−0.064	0.778*	0.437
	6	0.354	−0.257	0.777*	−0.083	0.753*	0.476
	7	0.392	−0.265	0.746*	−0.092	0.719*	0.519
RHU	0	0.104	0.162	−0.207	−0.168	−0.331	−0.363
	1	0.215	0.056	−0.133	−0.121	−0.317	−0.379
	2	0.178	0.065	0.027	−0.078	−0.332	−0.304
	3	0.174	0.073	0.079	−0.071	−0.348	−0.277
	4	0.193	0.115	0.100	−0.080	−0.364	−0.326
	5	0.231	0.074	−0.014	−0.069	−0.354	−0.287
	6	0.323	0.001	−0.038	−0.103	−0.355	−0.268
	7	0.335	−0.050	−0.091	−0.091	−0.349	−0.327
PRE	0	0.263	−0.059	0.615*	0.582*	0.650*	0.595*
	1	0.296	−0.134	0.556*	0.581*	0.645*	0.577*
	2	0.249	−0.115	0.625*	0.634*	0.637*	0.571*
	3	0.246	−0.119	0.709*	0.676*	0.633*	0.639*
	4	0.276	−0.125	0.733*	0.635*	0.622*	0.613*
	5	0.346	−0.095	0.679*	0.638*	0.614*	0.557*
	6	0.375	−0.155	0.748*	0.620*	0.609*	0.575*
	7	0.322	−0.147	0.635*	0.605*	0.592*	0.652*

Table 6

Lagged correlation coefficients at 0 to 7-days between the daily reported infected cases and temperature (TMP in °C), relative humidity (RHU in %) and precipitation (PRE in mm) over selected countries in the South America (* *significant at* $p \leq 0.05$; *bold value is an indicator of lagging*).

Parameters	Lag/days	Countries										
		Argentina	Brazil	Chile	Colombia	Guyana	Ecuador	Paraguay	Peru	Uruguay	Trinidad/Tobago	Venezuela
TMP	0	−0.682*	−0.724*	−0.731*	0.248	0.194	−0.144	−0.460	−0.910*	−0.300	0.042	0.122
	1	−0.709*	−0.715*	−0.753*	0.231	0.187	−0.124	−0.584*	−0.916*	−0.276	0.006	0.085
	2	−0.672*	−0.749*	−0.758*	0.239	0.215	−0.129	−0.599*	−0.910*	−0.285	−0.057	0.016
	3	−0.622*	−0.803*	−0.752*	0.237	0.202	−0.083	−0.512	−0.918*	−0.285	0.038	0.194
	4	−0.576*	−0.825*	−0.732*	0.218	0.234	−0.020	−0.316	−0.907*	−0.267	−0.010	0.195
	5	−0.609*	−0.816*	−0.717*	0.222	0.316	−0.074	−0.221	−0.884*	−0.204	0.000	0.156
	6	−0.611*	−0.814*	−0.727*	0.254	0.264	−0.116	−0.246	−0.859*	−0.205	−0.001	0.138
	7	−0.664*	−0.810*	−0.739*	0.272	0.203	−0.190	−0.253	−0.848*	−0.203	−0.101	0.067
RHU	0	0.315	−0.774*	0.148	−0.138	0.052	0.137	−0.181	−0.702*	0.471	−0.194	0.318
	1	0.365	−0.799*	0.219	−0.139	−0.009	0.100	−0.170	−0.684*	0.442	−0.146	0.392
	2	0.365	−0.747*	0.278	−0.163	−0.036	0.092	−0.009	−0.626*	0.501	−0.180	0.435
	3	0.346	−0.710*	0.204	−0.162	0.039	0.103	0.017	−0.569*	0.462	−0.199	0.276
	4	0.297	−0.691*	0.107	−0.136	−0.051	0.060	0.015	−0.580*	0.445	−0.128	0.234
	5	0.276	−0.684*	−0.008	−0.102	−0.042	−0.017	0.019	−0.596*	0.412	−0.110	0.250
	6	0.254	−0.672*	−0.050	−0.086	−0.093	−0.002	0.056	−0.505	0.462	−0.132	0.314
	7	0.278	−0.697*	−0.030	−0.127	−0.020	−0.038	0.029	−0.457	0.454	−0.124	0.357
PRE	0	−0.260	−0.493	−0.393	0.317	0.299	0.121	−0.364	−0.590*	0.185	0.059	0.394
	1	−0.273	−0.533*	−0.427	0.282	0.159	0.206	−0.407	−0.588*	0.106	0.009	0.380
	2	−0.243	−0.568*	−0.430	0.269	0.196	0.171	−0.359	−0.598*	0.098	−0.032	0.424
	3	−0.194	−0.591*	−0.410	0.294	0.322	0.113	−0.244	−0.569*	0.178	−0.042	0.416
	4	−0.139	−0.589*	−0.411	0.294	0.361	0.116	−0.100	−0.530*	0.185	−0.067	0.365
	5	−0.187	−0.570*	−0.439	0.310	0.318	0.130	−0.087	−0.493	0.130	−0.049	0.340
	6	−0.216	−0.552*	−0.488	0.319	0.174	0.073	−0.097	−0.448	0.023	−0.012	0.340
	7	−0.254	−0.531*	−0.509	0.314	0.155	0.034	−0.096	−0.418	0.179	−0.042	0.405

Spatial fluctuations in the global climatology revealed general decrease in temperature during the study period in the Arctic, Oceania, southern Africa and some parts of Europe, Asia, South and North America. However, increased temperature (warmer climate) was recorded in the South Pole and southern coast of South America. Conversely and as expected, relative humidity was found to increase in warmer regions and decreased in a colder region. Most regions of the world had a slight and insignifi-

cant increase or decrease in precipitation with exception of some parts of southern Asia with significant increase or decrease in precipitation.

Results revealed that the effects of daily variations in climate on the spread of COVID-19 infection varied from across different climatic regions of the world. We obtained both negative ($−0.510 \leq r \leq −0.967$) and positive ($0.519 \leq r \leq 0.999$) strong relationships (at $p < 0.05$) between climatic variables and con-
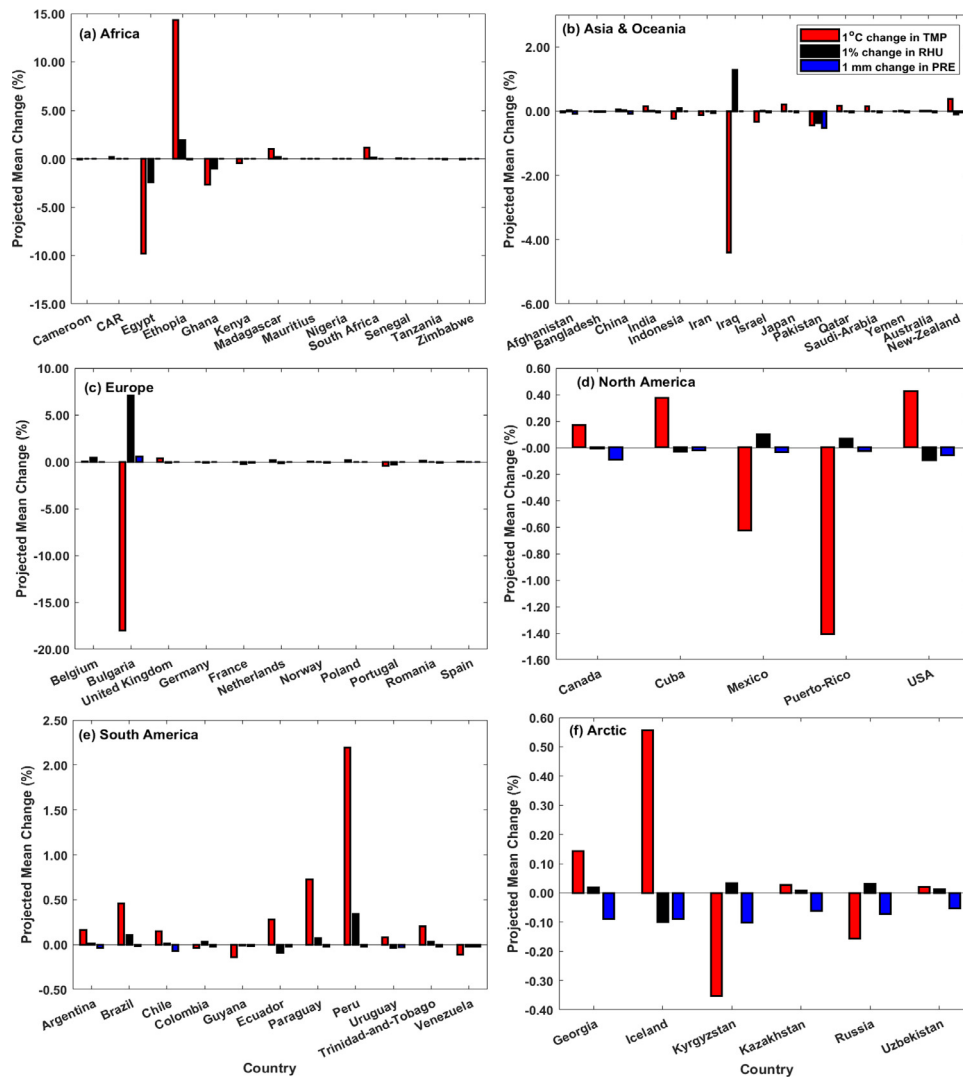
Fig. 6. Projected changes in COVID-19 infection with a unit change (decrease) in temperature (TMP), humidity(RHU) and precipitation (PRE) in different countries in (a) Africa, (b) Asia and Oceania, (c) Europe (d) North America, (e) South America, and (f) the Arctic Region from December 31, 2019 to May 28, 2020 at 12.00 GMT.

firmed cases of COVID-19 in about 42 (68.85%) of the selected countries. Temperature gave significant correlations in 49.2% of all the selected countries around the world (with 34.4% positive and 14.6% negative). Relative humidity showed positive and negative relationship in 0.08% and 44.26% of the countries respectively while precipitation produced 18.03% (positive) and 0.07% (negative). Méndez-Arriaga (2020) in Mexico found significant associations between the climate (positive for precipitation and negative for temperature) and the local transmission ratio of the disease. Our results showed that local transmission of the disease spanned all climatic zones i.e. from cold and dry to hot and humid regions as previously reported (O'Reilly et al., 2020; WHO, 2020) which was found to be triggered by travel patterns out of the high-risk countries (Lai et al., 2020). However, our results revealed no significant relationship between the climate and COVID-19 cases in 30.77% of countries in Africa (*i.e.* Central Africa Republic, Mauritius, Tanzania and Zimbabwe); 30.77% in Asia (Afghanistan, China, Israel, and Japan); 100% in Oceania (Australia and New Zealand); 27.27% in Europe (Spain, Portugal, Norway), 54.55% in South America (Colombia, Ecuador, Uruguay, Guyana, Trinidad and Tobago, and Venezuela), and 33.3% in the Arctic region (Georgia and Iceland). Briz-Redón and Serrano-Aroca (2020) in their spatio-temporal analysis for exploring the effect of temperature

on COVID-19 had also reported no significant association between variations in climate and the evolution of the disease in Spain. Possible reasons for these findings could be due to various factors such as variations in demographic, socioeconomic, cultural, the standard of healthcare, level of compliance with national policies on COVID-19 protocols to fight the pandemic. Furthermore, there were strong evidences of 1 to 7-day delays in the response of the infection to changes in climate. This is an indication that the effects of climate variations may take 1 to 7 days to manifest in an infected individuals or it may be a manifestation of the incubation period of COVID-19 infections, which is 2–14 days. Previous studies have reported that delayed response to diseases, which may however vary with victim's age, body characteristics and underlying health condition may adversely affect the turnout of victims in seeking medical treatment and that the condition may be dangerous in countries with poor testing rate (e.g. Tanimola et al., 2013)

Statistical model simulations suggested that one-degree Celsius fall in temperature could significantly increase COVID-19 infection in two (15.38%) African countries (Ethiopia and South Africa); three (60%) countries in North America (Canada, USA and Cuba); five (45.45%) countries in South America (Peru, Paraguay, Brazil, Trinidad and Tobago and Ecuador); and two (33.3%) countries in the Arctic region (Iceland and Georgia). One-degree fall in tem-

perature, however, projected significant decrease the infection in three (23.08%) countries in Africa (Egypt, Kenya and Ghana); one country, each, in Asia (0.07%; Iraq) and Europe (0.09%; Bulgaria); 2 countries, each, in North America (40.0%; Mexico, Puerto Rico); South America (18.2%; Guyana and Venezuela) and the Arctic region (33.3%; Kyrgyzstan and Russia). When the relative humidity falls by one-percent, it projected an increase in COVID-19 cases in one country, each, in Africa (7.69%; Ethiopia); Asia (7.69%; Iraq), and Europe (9.09%; Bulgaria); two in North America (40%; Mexico and Puerto Rico); three South America (27.27%; Peru, Paraguay and Brazil) and two in the Arctic region (33.33%; Kyrgyzstan and Russia). On the other hand, a decrease in the infection was predicted in two countries in Africa (18.18%; Egypt, and Ghana); one, each, in Asia (7.69%; Pakistan), North America (20%; USA), South America (9.09%; Ecuador) and the Arctic region (16.67%; Iceland) for a drop in relative humidity. A general reduction in COVID-19 cases was projected with a unit drop in precipitation in two countries in North America (40%; Canada and the USA), one, each, in Asia (7.69%; Pakistan) and South America (9.09%; Chile) and five in the Arctic region (83.33%; Kyrgyzstan, Iceland, Georgia, Russia and Uzbekistan). Wang et al. (2020a) had also reported that one-degree Celsius drop/rise in temperature could increase or reduce COVID-19 infection rate in China and the US while a 1% drop/rise in relative humidity could increase/reduce the spread of the disease. Our results, thus, confirmed the fact that the local transmission of the disease might not reduce significantly by the onset of warmer season/summer in the northern hemisphere. Similarly, the intensity of the infection might increase or reduce during the advancing winter in the southern hemisphere. As such effective public health interventions such as social distancing, wearing of face mask and frequent washing of hands with an alcohol-based sanitizer among others are crucial to containing the transmission of COVID-19.

5. Conclusion

We have assessed the potential effects of climate variations (humidity, temperature, and precipitation) on COVID-19 in different climatic zones of the world. Data used include daily records of COVID-19 (confirmed cases and deaths) in 61 selected countries well-distributed over six designated regions of the world (Africa, Asia & Oceania, Europe, North America, South America and the arctic region) from December 31, 2019 to May, 28 2020 (at 12.00 GMT). In addition, daily records of temperature, humidity, and precipitation obtained from high-resolution ($0.25°$ by $0.25°$) ERA5 datasets for the same period were used. The data were analysed using statistical and geo-statistical methods, including multiple linear regression model, correlation analysis and spatial gridding. Our findings revealed higher spread of the spatial distribution of the infections in the northern hemisphere (i.e. high latitudes, with temperate and/or continental climate) and the prominent direction of the transmission was more from the epicentre to the western countries. There were strong indications that the effects of variations in climate on the spread of COVID-19 infection were both negative ($-0.510 \leq r \leq -0.967$) and positive ($0.519 \leq r \leq 0.999$) and significant (at $p < 0.05$). The impacts varied across different climatic regions of the world. There were also evidence of 1 to 7-day lagging in the response of the infection to changes in weather. The model simulations suggested that one-degree Celsius fall in temperature could significantly increase COVID-19 infection in 19.67% of the selected countries of the world but projected a decrease in other 18.03%. Similarly, one unit drop in relative humidity could upsurge COVID-19 infection in 16.39% of the countries but a decrease in 0.1%. However, a decrease in a unit precipitation was expected to generally reduce the infection in 14.75% countries. The findings had revealed that local transmission of the disease in

both the northern and southern hemispheres might not shrink during the summer months. As such, public health interventions like social distancing, wearing of face mask and frequent washing of hands with soap or alcohol-based sanitizers are crucial to controlling the transmission of COVID-19 in all seasons. This paper has improved our knowledge of the spread of COVID-19 by showing that warm, wet and humid climates could significantly influenced the spread of the disease. However, climatic factors are not the only variables responsible for the observed variations in the disease transmission. Further areas of research can look at the effects of climate on the spread of the disease while controlling for other factors that can affect transmissibility such as adherence to COVID-19 control measures, international travels and population densities.

Declaration of Competing Interest

None.

Supplementary materials

Supplementary material associated with this article can be found, in the online version, at doi:10.1016/j.sste.2021.100417.

References

Araujo, M.B., Naimi, B., 2020. Spread of SARS-CoV-2 Coronavirus likely to be constrained by climate. MedRxiv.

Bashir, M.F., Ma, B., Shahzad, L., 2020. A brief review of socio-economic and environmental impact of Covid-19. Air Qual. Atmos. Heal. doi:10.1007/s11869-020-00894-8.

Bernauer, W., Slowey, G., 2020. COVID-19, extractive industries, and indigenous communities in Canada: notes towards a political economy research agenda. Extrac. Indust. Soc. doi:10.1016/j.exis.2020.05.012.

Brooks, S.K., Webster, R.K., Smith, L.E., Woodland, L., Wessely, S., Greenberg, N., Rubin, G.J., 2020. The psychological impact of quarantine and how to reduce it: rapid review of the evidence. Lancet 395, 912–920.

Briz-Redón, Á., Serrano-Aroca, Á., 2020. A spatio-temporal analysis for exploring the effect of temperature on COVID-19 early evolution in Spain. Sci. Total Environ., 138811.

Chan, J.F., Yuan, S., Kok, K.H., To, K.K., Chu, H., Yang, J., et al., 2020. A familial cluster of pneumonia associated with the 2019 novel coronavirus indicating person-to-person transmission: a study of a family cluster. Lancet 2020. doi:10.1016/S0140-6736(20) 30154-9, PubMed PMID:31986261 .

Chakrabarti, S.S., Kaur, U., Banerjee, A., Ganguly, U., Banerjee, T., Saha, S., et al., 2020. COVID-19 in India: are biological and environmental factors helping to stem the incidence and severity? Aging Dis. 11 (3), 480–488. doi:10.14336/AD.2020.0402.

Collivignarelli, M.C., Abbà, A., Bertanza, G., Pedrazzani, R., Ricciardi, P., Miino, M.C., 2020. Lockdown for CoViD-2019 in Milan: what are the effects on air quality? Sci. Total Environ. 732, 139280.

Conticini, E., Frediani, B., Caro, D., 2020. Can atmospheric pollution be considered a co-factor in extremely high level of SARS-CoV-2 lethality in northern Italy? Environ. Pol. 114465. doi:10.1016/j.envpol.2020.114465.

Copernicus Climate Change Service (C3S), 2017. ERA5: Fifth Generation of ECMWF Atmospheric Reanalyses of the Global Climate. Copernicus Climate Change Service Climate Data Store (CDS) Accessed on April 15, 2020. https://cds.climate.copernicus.eu/cdsapp#!/home.

Davis, J.C., 1986. Statistics and Data Analysis in Geology. John Wiley & Sons, London, UK.

de Smith, M.J., Goodchild, M.F., Longley, P.A., 2018. Geospatial Analysis: a Comprehensive Guide to Principles Techniques and Software Tools, sixth ed. Winchelsea Press, New York, USA.

Di Pietro, R., Basile, M., Antolini, L., Alberti, S., 2020. Genetic drift and environmental spreading dynamics of COVID-19. MedRxiv.

Fattorini, D., Regoli, F., 2020. Role of the chronic air pollution levels in the Covid-19 outbreak risk in Italy. Environ. Poll., 114732.

Feng, C., Wang, H., Lu, N., Chen, T., He, H., Lu, Y., Xin, M., Tu, X.M., 2014. Log-transformation and its implications for data analysis. Shanghai Arch. Psychol. 26 (2), 105–109. doi:10.3969/j.issn.1002-0829.2014.02.009.

Fofana, N.K., Latif, F., Sarfraz, S., Bilal, Bashir, M.F., Komal, B., 2020. Fear and agony of the pandemic leading to stress and mental illness: an emerging crisis in the novel coronavirus (COVID-19) outbreak. Psychiatry Res., 113230.

Gautam, S., 2020. COVID-19: air pollution remains low as people stay at home. Air Qual. Atmos. Heal. 13, 853–857. doi:10.1007/s11869-020-00842-6.

Geoghegan, J.L., Holmes, E.C., 2017. Predicting virus emergence amid evolutionary noise. Open Biol. 7, 170189.

Hammer, Ø., Harper, D.A.T., Ryan, P.D., 2001. PAST: paleontological statistics software package for education and data analysis. Palae. Electron. 4 (1), 1–9.

Knowland, E.K., Keller, C., Ott, L., Pawson, S., Saunders, E., Wales, P., Duncan, B., 2020. Local to global air quality simulations using the NASA GEOS composition forecast model. GEOS-CF.

Kraemer, M.U.G., Golding, N., Bisanzio, D., Bhatt, S., Pigott, D.M., Ray, S.E., et al., 2019. Utilizing general human movement models to predict the spread of emerging infectious diseases in resource poor settings. Sci. Rep. 9, 5151. doi:10.1038/s41598-019-41192-3.

Lai, S., Bogoch, I., Ruktanonchai, N.W., Watts, A., Lu, X., Yang, W., Yu, H., Khan, K., Tatem, A.J., 2020. Assessing spread risk of Wuhan novel coronavirus within and beyond China, January–April 2020: a travel network-based modelling study. medRxiv 2020; published March 9. DOI:10.1101/2020.02.04.20020479 (preprint).

Li, Q., Guan, X., Wu, P., Wang, X., Zhou, L., Tong, Y., et al., 2020. Early transmission dynamics in Wuhan, China, of novel coronavirus-infected pneumonia. N Engl. J. Med. doi:10.1056/NEJMoa2001316, PubMed PMID:31995857.

Méndez-Arriaga, F., 2020. The temperature and regional climate effects on communitarian COVID-19 contagion in Mexico throughout phase 1. Sci. Total Environ., 139560.

Mishra, A.K., Wargocki, P., 2020. Understanding the spread of SARS-CoV-2: associations between the number of cases in regions and selected economic and geographic parameters. ArXiv Preprint ArXiv: 2004.00110.

O'Reilly, K.M., Auzenbergs, M., Jafari, Y., Liu, Y., Flasche, S., Lowe, R., 2020. Effective transmission across the globe: the role of climate in COVID-19 mitigation strategies. Lancet Planet Health. doi:10.1016/S2542-5196(20)30106-6, published online May 6.

Rodríguez-Barranco, M., Tobías, A., Redondo, D., Molina-Portillo, E., Sánchez, M.J., 2017. Standardizing effect size from linear regression models with log-transformed variables for meta-analysisBMC. Med. Res. Methods 17, 44. doi:10.1186/s12874-017-0322-8.

Sahu, K.K., Mishra, A.K., Lal, A., 2020. COVID-2019: update on epidemiology, disease spread and management. Monaldi Arch. Chest Dis. 90 (1292), 197–205.

Sajadi, M.M., Habibzadeh, P., Vintzileos, A., Shokouhi, S., Miralles-Wilhelm, F., Amoroso, A., 2020. Temperature, humidity and latitude analysis to predict potential spread and seasonality for COVID-19. SSRN 2020. published online March 5. https://ssrn.com/abstract=3550308. (preprint).

Sharif, A., Aloui, C., Yarovaya, L., 2020. COVID-19 pandemic, oil prices, stock market, geopolitical risk and policy uncertainty nexus in the U.S. economy: fresh evidence from the wavelet-based approach. Inter. Rev. Fin. Anal. 70, 101496. doi:10.1016/j.irfa.2020.101496.

Tanimola, M., Hamilton, W., Ukoumunne, O.C., 2013. Ethnic inequalities in time to diagnosis of cancer: a systematic review. BMC Fam. Pract. 14 (1), 197–205.

Wang, J., Tang, K., Feng, K., Lin, X., Lv, W., Chen, K., Wang, F., 2020a. High temperature and high humidity reduce the transmission of COVID-19. SSRN 2020. published online March 9. https://ssrn.com/abstract=3551767. (preprint).

Wang, P., Chen, K., Zhu, S., Wang, P., Zhang, H., 2020b. Severe air pollution events not avoided by reduced anthropogenic activities during COVID-19 outbreak. Resour. Conser. Recycl. 158, 104814. doi:10.1016/j.resconrec.2020.104814.

World Health Organization (WHO), 2020. Novel coronavirus (2019-nCoV) https://www.who.int/emergencies/diseases/novel-coronavirus-2019. Accessed 30 January 2020.

Zar, J.H., 1992. Biostatical Analysis, second ed. Prentice-Hall, Eaglewood Cliffs, NJ.

Zhu, Y., Xie, J., Huang, F., Cao, L., 2020. Association between short-term exposure to air pollution and COVID-19 infection: evidence from China. Sci. Total Environ. 727, 138704. doi:10.1016/j.scitotenv.2020.138704.